Magnetoresistance induced by spin transfer torque in electrodeposited granular multilayers based on Co/Zn system

P. PASCARIU*, V. GEORGESCU
Faculty of Physics "Al. I. Cuza" University, Iaşi 700506, Romania

In this work we study transfer of spin angular momentum across multilayered granular films composed of ferromagnetic (Co)/diamagnetic (Zn) metals. Magnetoresistance (MR) and spin transfer torque phenomena (STT) were studied for two series of multilayers labeled $[Co/Zn]_n$ and $[Zn/Co]_n$, starting with Co and Zn layers, respectively, electrolitically grown onto Cu (100) substrate under identical conditions. The coercivity varied between (145Oe÷208Oe) as a function on the Zn layer thickness, with largest values for the samples starting with Co. The $[Co/Zn]_n$ and $[Zn/Co]_n$ electrodeposited multilayers display magnetoresistance (14%) effect which can be explained mainly by the exchange interaction among neighbouring layers and by the spatially inhomogeneous magnetic structure of the granular multilayer (favoring spin scattering at interfaces between grains and layers); in addition, the thickness of the Zn interlayer has an important role on the transportation and diffusion processes.

(Received June 30, 2011; accepted August 10, 2011)

Keywords: Electrodeposition, Co/Zn multilayers, Structural properties, Magnetic properties, Giant magnetoresistance (GMR)

1. Introduction

Research on metallic multilayers is a topic of major interest, especially since the discovery of the giant magnetoresistance (GMR) effect in magnetic/nonmagnetic multilayers with the thickness of the individual layers in the nanometer range [1, 2]. It was shown that significant GMR values can be achieved in granular heterogeneous alloys or granular multilayer [3-7].

On the other hand, as predicted Berger [7] and Slonczewski [8], a spin polarized current can transfer its angular momentum to a ferromagnet, inducing a torque on its magnetization (it was later established experimentally [9-12]). Thus, the magnetic moment can switch to another state or oscillate around its equilibrium position at microwave frequencies; this phenomenon is called spin transfer torque. We considered that it is very interesting to study such phenomena in granular multilayered thin films. It is known that granular solids with nanometer size magnetic granules have a higher density of interfaces, which can potentially lead to a larger GMR [3, 4].

The present work deals with the study of magnetic and magnetotransport properties of Co/Zn granular multilayers in a view to foresee some technological applications; especially, we envisaged the spin transfer torque phenomena (STT) in such multilayers. A first reason for selecting the Co/Zn system is that we expected the formation of granular structure with sharp interfaces between the Zn and the Co-rich zones due to immiscibility of the constituents under equilibrium conditions. Since both zinc (diamagnetic) and cobalt (ferromagnetic) are immiscible elements on a large scale of concentration, as derived from their phase diagram [13], this factor can lead to production of granular materials. Another reason is that diamagnetic materials cause lines of magnetic flux to curve away from the material. The ferromagnets (which have a permanent positive moment) and paramagnets (which induce a positive magnetic moment) are attracted to magnetic field maxima, and diamagnets (which induce a negative moment) are attracted to field minima. We suppose that this behavior could produce some peculiarities in magnetic flux lines distribution in multilayered Co/Zn granular samples, favoring the antiferromagnetic (AF) coupling between neighboring layers, and as consequence the magnetoresistance should be enhanced. This type of AF coupling could be dependent on the layer thickness and on the interface between layers or granules.

We prepared by electrodeposition two series of granular multilayers labeled $[Co/Zn]_n$ and $[Zn/Co]_n$, starting with Co or Zn layers, respectively. We studied the effects of the seed layer (Co or Zn) and of the Zn layer thickness concerning the properties of multilayer. Magnetic and magnetotransport properties of the samples were measured and discussed in correlation with morphology. As far as we know of, this is the first time when Co/Zn multilayered granular films have been fabricated by electrodeposition and their magnetic and magnetotransport properties were studied.

2. Experimental

The samples studied in this work were prepared by electrodeposition in potentiostatic regime, by using dual baths method [14]. A holder system with three electrodes was introduced alternately in the two baths for electrodeposition of Zn or Co. Electrodeposition was performed in potentiostatic regime, using a holder system with three electrodes, by using platinum anode and a platinum wire as quasi-reference electrode (the contact area with solution was of 0.06 mm^2). The disk-shaped cathode (20 mm in diameter) was made from (100)-textured polycrystalline copper foils. The solutions for Zn or Co layer plating contained: Zn in the form of zinc (II) sulfate, Co in the form of cobalt (II) sulfate and the additional substances (H_3BO_3, NaCl, $Na_2SO_4 \cdot 10H_2O$, and triethanolamine ($(CH_3CH_2OH)_3N$), which were the same for both baths. Electrodeposition was carried out at 3.0 V bias voltages for both electrolytic baths and the solution *pH* was kept constant at 4.0, without stirring the electrolyte. The copper substrates were surfaced prior to electroplating by abrasion with emery powder, etching in dilute HNO_3, and washing in distilled water. The system of electrodes was alternatively introduced in each bath, controlling the time of immersion; before each immersion in electrolytic baths, the system was carefully rinsed in distilled water. To avoid co-deposition of Co-Zn alloy in the same layer, we chose the dual-bath technique for electrodeposition that offers some advantages for the sample production comparative with single-bath technique. Indeed, the application of electrolyte components and the adjustment of their concentration can be independent of each other, and the magnetic layer can be void of the non-magnetic element.

The nominal thicknesses of the Co and Zn layers were estimated from the consumed charge, the rate of electrodeposition being established by depositing some thick (500 nm) films of Co and Zn in the same conditions as those used for multilayer electrodeposition. The weights of the deposits were measured for these thick films by means of a microbalance with an error of $\pm 10^{-6}$ g. In addition, a MII-4 Linnik interferential microscope was used to measure the thickness of these films by the multiple-beam Fizeau fringe method, at reflection of monochromatic light. The deposition rates of Co and Zn layers were calculated as 0.3 and 0.7nm/sec, respectively.

We have prepared by this procedure two series of $[Co/Zn]_n$ and $[Zn/Co]_n$ multilayers, (starting with Co or Zn layers) with different thicknesses of Zn layers , varying in the range (t_{Zn}=0.8÷5.0)nm, under otherwise identical conditions and containing stacks of n=50 periods. The thickness (t_{Co}) of the Co layers in multilayered structures was maintained constant at 5.0 nm. The notation of these samples is as follows (with layer thickness expressed in nm):

1. Multilayers starting with Co layer: S1 [Co(5.0)/Zn(5.0)], S2 [Co(5.0)/Zn(2.6)] and S3 [Co(5.0)/Zn(0.8)]
2. Multilayers starting with Zn layer: S4 [Zn(5.0)/Co(5.0)], S5 [Zn(2.6)/Co(5.0)] and S6 [Zn(0.8)/Co(5.0)]

The surface morphology experiments were performed by atomic force microscopy in the tapping mode (using WSXM software for scanning probe microscopy) [15].

The magnetic measurements were carried out using an induction type device with the *ac* magnetic field applied in the film plane (50 Hz, in a maximum field of 750 *Oe*) at room temperature.

The resistance measurements were performed at room temperature by using a particular type of device with a current flowing perpendicular to the film plane ($I = \pm 1$ A), between the Cu substrate on which is deposited granular film and a gold wire contact, spring pressed on the top surface of the film. In such a way, the current lines flow from the surface of the Cu bottom disc to the top layer, traversing simultaneously through the entire volume of the multilayered granular film. Resistance $R=V/I$ was measured at room temperature as a function of current I and magnetic field H, by using a programmable digital instrument. The shunt effect of the substrate was not corrected. The variable external magnetic field with a maximum value of $H=\pm$ 4420 Oe was applied in the film plane.

3. Results and discussion

We performed firstly the measurements by atomic force microscopy in order to investigate both the effect of the seed layer (Co or Zn) and of the Zn layer thickness on film morphology, for the series of multilayers starting with Co or Zn, having varied Zn layer thicknesses.

For a brief presentation of experimental results on the two series of samples we chose as example for figures in this study the following representative samples: S1-$[Co(5)/Zn(5)]_{50}$, S3-$[Co(5)/Zn(0.8)]_{50}$ which are samples starting with a Co layer and S4-$[Zn(0.8)/Co(5)]_{50,}$ S6-$[Zn(5)/Co(5)]_{50}$ which are samples starting with a Zn layer.

Fig. 1 shows two-dimensional AFM images of the surface morphology of some Co/Zn granular multilayered films (starting with Co layers), comprising 50 stacks of alternating Co layers (t_{Co}=5 nm) and Zn layers (t_{Zn}=0.8-5 nm) grown on a (100) Cu substrate. Topographic AFM images (left side column, a and c) as well as the corresponding phase images (right side column, images b, d) are shown for the samples: S1 [Co(5.0)/Zn(5.0)] (a, b) and S3 [Co(5.0)/Zn(0.8)] (c, d).

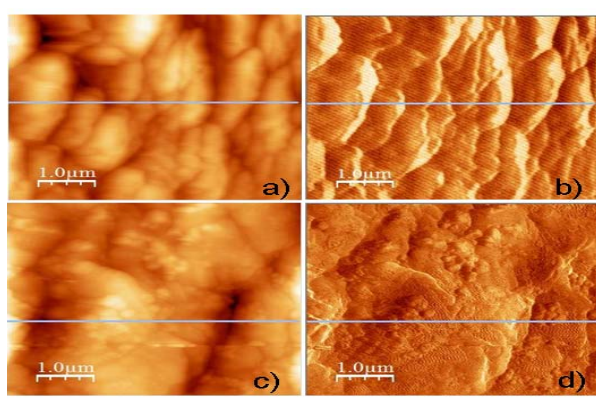

Fig. 1. AFM surface topography (left side column) and the corresponding phase images (in the right side column) for the samples: S1 (a, b), S3 (c, d). The scan area is 5×5 μm^2.

Fig. 2 shows two-dimensional AFM images of the surface morphology of two Zn/Co granular multilayered films (starting with Zn layers). Topographic AFM images (left side column, a, c) as well as the corresponding phase images (right side column, images b, d) are shown for the samples: S4 [Zn(5.0)/Co(5.0)] (a, b) and S6 [Zn(0.8)/Co(5.0)] (c, d).

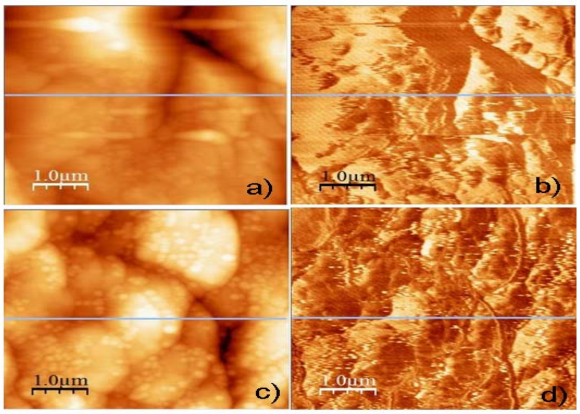

Fig. 2. AFM surface topography (left side column) and the corresponding phase images (in the right side column) for the samples: S4 (a, b), S6 (c, d). The scan area is 5×5 µm^2.

From the general examination of these images, it is obvious that both $[Co/Zn]_{50}$ and $[Zn/Co]_{50}$ were grown by a progressive nucleation mechanism with formation of tridimensional insular grains. The increase of the Zn layer thickness determines an increase in size and density of insular nanocrystalline grains as it is shown by comparison between topography images of the samples S3, S1 and S6, S4, for [Co/Zn] and [Zn/Co], respectively.

For the series of samples electrodeposited with different Zn layer thicknesses, the roughness parameter – root mean square (*RMS*) – was calculated from the 5 µm×5 µm AFM topography scan as follows: (S1) 84.49 nm, (S3) 105.21 nm, (S4) 162.80 nm and (S6) 106.88 nm. From the AFM analyses (Fig. 2) we found out that the more the Zn layer thickness increases, the multilayer being started with Zn, the larger the roughness becomes, inversely than in the case of films starting with a Co layer (Fig. 1).

When we studied the two groups of samples, where the Zn layer thickness is decreased: S1 [Co(5.0)/Zn(5.0)], S3 [Co(5.0)/Zn(0.8)], in the case of multilayers starting with Co layer and S4 [Zn(5.0)/Co(5.0)], and S6 [Zn(0.8)/Co(5.0)] for those starting with Zn, we have had in mind that the effect of decreasing t_{Zn} results in increasing strength of interaction between magnetic layers. The relation between the size of the grains in granular multilayers and the nominal layer thickness is generally determined by the three-dimensional growth process. The average diameter of the grains can be much larger than the nominal layer thickness, depending on the material parameters e.g., lattice parameter mismatch, surface energy, etc., as well as various electrodeposition parameters. The increase of the Zn spacer layer thickness from 0.8 to 5.0 nm was found to decrease the magnetic grain size both in Co/Zn and Zn/Co granular multilayer samples. For samples S3 and S6 where the spacer layer thickness is 0.8 nm the magnetic grain size is increased, therefore it is most probable to have an increasing number of the pinholes and discontinuities of the Zn spacer.

It is known that the phase imaging provides complementary information to the topography image, revealing the variation in the surface properties. In Fig. 3 we show the phase profiles (a, b) of the images from figure 1 (taken along the marked x-y line), and the corresponding cross-section topographic profiles (c, d) for the following multilayers starting with a Co layer: S1 [Co(5.0)/Zn(5.0)] (a, b) and S3 [Co(5.0)/Zn(0.8)] (c, d).

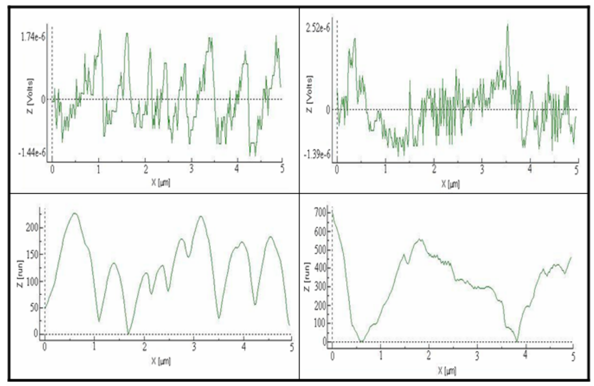

Fig. 3. Phase profiles (a, b) of the images shown in Fig. 1 (taken along the marked x-y line), and the corresponding cross-section topographic profiles (c, d) for the following multilayers starting with a Co layer: S1 [Co(5.0)/Zn(5.0)] (a, b) and S3 [Co(5.0)/Zn(0.8)] (c, d).

The phase shift angle of an oscillating cantilever is sensitive to tip-surface interactions, which is basically material specific. There are many surface properties that may have an effect on the phase shift contrast. They can be different surface compositions on a surface, differences in friction, viscoelasticity, adhesion, material, etc. We consider that the phase shift contrast in tapping mode AFM in our experiments can be used to distinguish different surface compositions on the surface, related to multilayered granular structure of the samples. As can be seen in Fig. 3, the cross section topography profiles of the samples S1 (in the left side) and S3 (in the right) show large grains with diameters in the µm range (Fig. 3 c, d). The phase imaging provides for clearer observation of fine features produced by multilayered structure in the case of two samples starting with Co layer and comprising larger Zn layers (5 nm for the sample S1) and (0.8 nm for the sample S3). The phase contrast images highlight the two-component structure of the [Co/Zn] multilayers. The brighter areas may be Zn grains with a periodicity larger for S1 than for S3 (Fig. 3c, d). The same features are observed also for the samples of [Zn/Co] multilayers.

The shape and slope of the in plane magnetization curves should depend on the nature of the first electrodeposited layer and on the Zn layers thickness, because the film morphology changes as a result of changing these preparation conditions.

Fig. 4a and Fig. 4b show the hysteresis cycles of the samples S1 and S3 with t_{Zn}=5 nm and t_{Zn}=0.8 nm, starting with Co. Fig. 4c and Fig. 4d show the hysteresis loops of two samples starting with Zn, S4 and S6, with the Zn layer thickness t_{Zn}=5 nm and t_{Zn}=0.8nm, respectively. We obtained the coercivity of maximum value (H_c *=208 Oe*) for the sample S1 and of minimum value (H_c *=173 Oe*) for the sample S3, respectively. The remanence was of about 1 ($M/M_s \approx 1$) for the sample S1 and of about 0.74 ($M/M_s \approx 0.74$) for the sample S3; this feature is indicative of ferromagnetic (FM) type coupling between the Co layers. The loop shapes for the multilayers (starting with Zn) are approximately similar. The coercivity of the sample S4 is of about *145 Oe,* while the remanence is $M/M_s \approx 0.55$. For the sample S6, the coercivity is *175 Oe* and the remanence is $M/M_s \approx 0.83$. All the samples show low-field hysteresis, from which we conclude that there is some degree of FM coupling in all the samples. We may conclude from these experiments that, by keeping the same thickness of the Co layer (t_{Co}=5 nm) in the multilayered structure, the magnetic behavior is much influenced by the Zn layers thickness and also by the first electrodeposited layers nature.

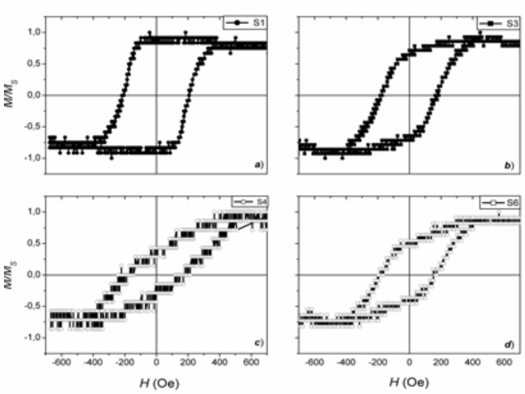

Fig. 4. Comparison between hysteresis loops recorded for the multilayers S1, S3 (starting with Co) and S4, S6 (starting with Zn).

To explain this behavior, we point out that the coercive field and easy magnetization axis are influenced from some specific features of granular multilayers. Generally, the local crystallographic directions changes when passing through a grain boundary. The normal components of the magnetization vectors of the two grains adjacent to boundary are not usually equal at remanence and this creates magnetic poles at grain-boundary. The local fields associated with these poles are sufficiently large, to cause reverse-domain creation at the grain boundary. The tensile stress caused by a lattice misfit could produce a common axis of easy magnetization despite the varied grain orientation. The dynamics of these complicated structures in our heterogeneous magnetic granular multilayers results in such various shapes of hysteresis cycles.

The magnetic susceptibility curves are shown in Fig. 5 for the samples: (a) S1 and S4, (b) S3 and S6.

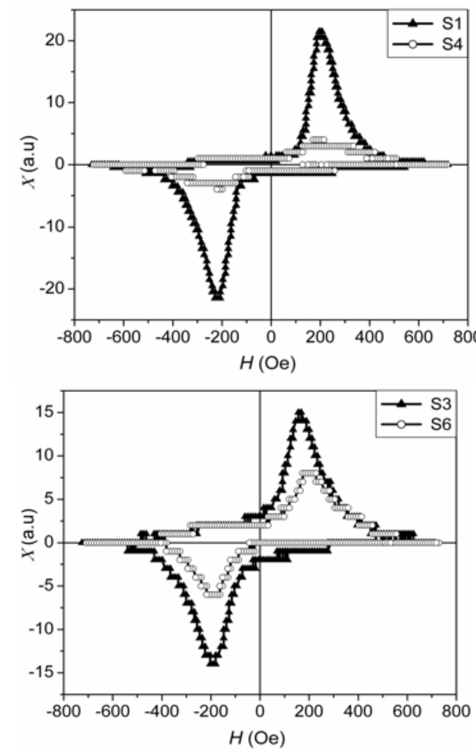

Fig. 5. Magnetic susceptibility curves of electrodeposited [Co/Zn] and [Zn/Co] multilayers for the samples: a) S1, S4 and b) S3, S6.

These smeared curves indicate a broad grain size distribution, but interactions between the grains are also likely to play a role as the Zn layer thickness decreases. The switching field distribution SFD=$\Delta H/H_c$, where ΔH is the full width at half maximum of the differential susceptibility χ=dM/dH, near H_c is a measure of the transition fluctuations that could be very important for granular films. We obtained the SFD of maximum value (SFD =1.260) for the sample S3 and of minimum value (SFD =0.746) for the sample S1, respectively. The SFD of the sample S4 is of about 0.940 and 1.078 for the samples S6.

The measurements of resistance versus applied d.c. magnetic field were performed by using the device described in experimental part of the paper. The magnetoresistance was defined as:

$$MR(\%) = \frac{R_0 - R_{I_{max}}}{R_{I_{max}}} X100 , \quad (1)$$

where R_0 is the film resistance measured in the lowest value of the current intensity, and R_{Imax} is the resistance in the maximum applied current intensity; I_0 = 0.01A and I_{max} = 1A for this experiment.

The curves *R(H)* plotted for two values of the bias current *I* applied perpendicular to the film plane (0.2A and 0.8A) are shown in Fig. 6, for the sample S1 (starting with Co) and the sample S4 (starting with Zn).

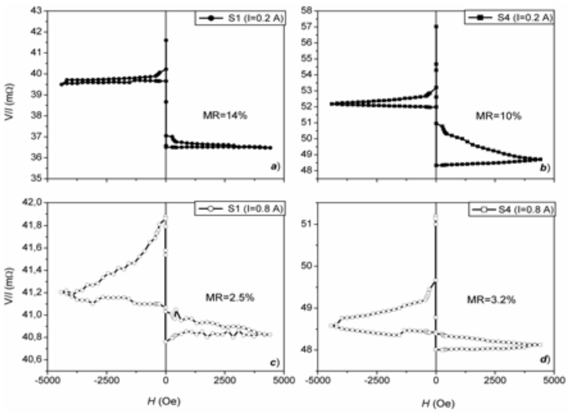

Fig. 6. Resistance vs. applied magnetic field for the samples S1 (a, c) and S4 (b, d) considered for various values of the current applied perpendicular to the film plane: I=0.2 mA (a, b), and I=0.8mA (c, d).

Fig. 7 shows the variation of the resistance with the current intensity exemplified for three values of the magnetic field applied in the film plane (H=270 Oe, 450 Oe, 1350 Oe), for the samples S1 [Co(5.0)/Zn(5.0)] and S4 [Zn(5.0)/Co(5.0)].

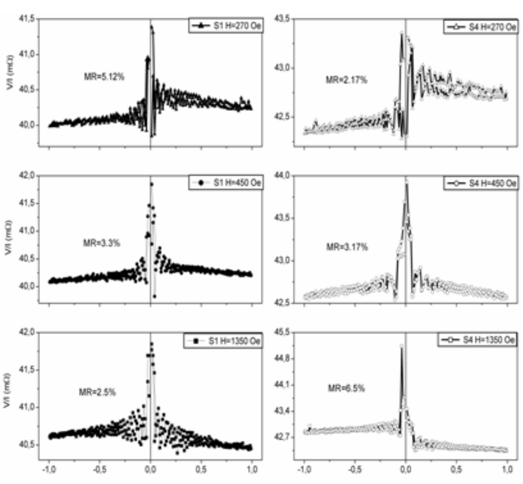

Fig. 7. V/I vs. current I for the samples S1 (left side column) and S4 (right side column) at different magnetic fields applied in the film plane: H=270 Oe (a), H=450 Oe (b), and H=1530 Oe (c).

The magnetic behavior of our granular multilayered films is more or less similar to that shown in plots from this figure, for all the samples. Two main features of the curves shown in Fig. 6 and 7 are peculiar: their asymmetry referring to the sign of magnetic field and the electric current influence exerted on multilayer magnetoresistance.

While magnetoresistance (MR) has generally been found to be symmetric in applied field in nonmagnetic or magnetic metals, we have observed asymmetric MR in Zn/Co multilayers, evidenced from the curves in Fig. 6.

In Fig. 6 we show the *R(H)* curves for two values of bias current *I*, for one complete cycle of the magnetic field from zero to ±4420 Oe. The resistance increases with the decrease of *I*, the MR values increase also (see values marked on the figure), and the area of the MR hysteresis cycle decreases. The samples in both series of $[Zn/Co]_{50}$ and $[Co/Zn]_{50}$ granular multilayered films display an asymmetric giant magnetoresistance effect (referring to the sign of applied magnetic field) and the area of the cycle. The values of CPP magnetoresistance are ranged between 10% for the samples S4 and 14.0% for the samples S1. We suppose that the asymmetry of magnetoresistance could be ascribed to spin polarization effects. The differences between the resistance values at positive and negative saturation fields could be ascribed to Lorenz force acting on the moving charge. The reorientation of magnetic cluster moments comprised in granular multilayered films could be due to electron spin-dependent scattering occurring in the magnetic Co clusters as well as at the Co/Zn and Zn/Co interfaces; the most important mechanism seems to be interfacial spin-dependent scattering [5, 6]. The appearance of the observed (*H*) asymmetry can be associated also with the existence of superparamagnetic entities in very small granules, like in the case of $Ni_{83}Fe_{17}/Cu$ system [16]. The hysteresis observed in the *R(H)* plots is an indicative of metastable state in domain formation of Co layers.

We marked on the Fig. 7 the values of resistance variation due to current (in constant magnetic field). We explain the influence of electric current *I* passing through the multilayered structure on the magnetoresistance values as an effect of spin transfer phenomena, analogous with [8]. The electrical current can transfer angular momentum to a ferromagnetic layer by spin transfer. For CPP geometry it was shown [8] that the spin-polarized nature of the current creates a mutual transference of spin angular momentum between the magnetic layers which is manifested in their dynamic response. For each pass of *H* through zero, the multilayer switch to the anti-parallel state of magnetic layers (high-resistance state) and then back to the parallel state (low-resistance state) at high field. The resulting effect of spin transfer phenomena and Lorentz force on moving electrons is increased when the bias current intensity is increased; this behavior results in different *R(H)* curves for different bias current, and different *R(I)* curves for different magnetic field, therefore in a resistance change dependent on the bias current and magnetic field.

Spin-polarized currents exert torque on magnetization that can switch the magnetization direction once the current density becomes sufficiently high. Taking into account only the ideal geometrical area of the film surface and neglecting the effect of the granular multilayer roughness (which increase very much the effective surface area), the calculated maximum density of current (J= 0.318 A/cm^2) is much lower than the critical-current density J_c required for current-driven switching in our films. This current-driven magnetization switching has been demonstrated on a number of metallic current-perpendicular-to-plane giant magnetoresistance (CPP-GMR) pillars [9, 10, 17–21] which exhibit magnetoresistance ratio of 0.5 –5%. The critical current density (J_c) of these devices varies from mid 10^6 to 10^8 A/cm^2 depending on the employed structure. In our case, spin-polarized currents exert a torque on magnetization, that modifies the magnetization direction insufficient to switch magnetization in opposite direction, but sufficient to influence the behavior of magnetic moments in the film, therefore the film magnetotransport features.

The Zn interlayer thickness plays a significant role on the magnetoresistance effects. The largest values for MR and R_c were obtained in the case of [Co/Zn]$_{50}$ multilayers with 5nm thickness of Zn layers. For these multilayers, the granular morphology (Fig. 1a, b) is well marked, the switching field distribution has the lowest value and coercive field has the largest value from the two series of studied samples. These correlations could suggest the way to obtain multilayers with properties convenient for technological applications.

4. Conclusions

The electrochemical deposition of Co/Zn and Zn/Co multilayered thin films was reported. The Co/Zn multilayered thin films were deposited from a sulfate bath solution by a two baths procedure. Using the control of the electrodeposition chemistry, *pH*, current density and temperature, [Co/Zn]$_{50}$ multilayered films with good magnetic properties were obtained.

The morphology and magnetic properties of the [Co/Zn] and [Zn/Co] depend strongly on the multilayer design, i.e. on the thicknesses of the Zn and Co layers, and on the seed layer (the first layer deposited onto Cu substrate). We studied the effect of the nominal thickness of individual Co and Zn layers and of the first electrodeposited layer in the film on the magnitude and behavior of GMR.

Comparing the shapes of the hysteresis loops, we have found that the magnetic features are very different, depending on the Zn layers thickness in multilayers. Although the total thickness of the Co layers (t_{Co}=250 nm) is the same for all studied samples, the hysteresis loops display various shapes, depending on the Zn layer thickness and on the nature of the first electrodeposited layer. This behavior is a result of the nucleation and growth processes of multilayers composed of immiscible elements, revealed by AFM topography and phase images.

The transfer of spin angular momentum across multilayered granular films composed of ferromagnetic (Co)/diamagnetic (Zn) metals was studied by using an electrical current flowing perpendicular to multilayered structure in the presence of magnetic field and it was revealed by variation in the multilayer magnetoresistance. The magnetoresistance values varied with the Zn layer thickness. The giant magnetoresistance contribution was of 14% for the Zn layer thickness t_{Zn}=5 nm (sample S1 [Co(5nm)/Zn(5nm)]$_{50}$ and of about 10% for the samples starting with Zn as seed layer (samples S4 [Zn(5nm)/Co(5nm)]$_{50}$, respectively. The increase in the GMR effect is attributed to spin polarization effects. The large enhancement is explained by scattering of the spin polarized conduction electrons on diamagnetic grains.

Acknowledgement

This work was partially supported by the Ministry of Education, Research, Youth and Sport and by the Social European Funds provided through Project 5244 No. RO08- POSDRU- 6/1.5/S/25. The authors are grateful to Lect. dr. Cristian Pirghie Department of Mechanical Engineering, "Stefan cel Mare" University, 720225 Suceava, Romania for the AFM measurements.

References

[1] M. N. Baibich, J. M. Broto, A. Fert, F. Nguyen Van Dau, F. Petroff, P. Etienne, G. Creuzet, A. Friederich, V. Chazelas, Phys. Rev. Lett., **61**, 2472 (1988).
[2] P. Grünberg, Acta Mater. **48**, 239 (2000).
[3] E. E. Fullerton, M. J. Conover, J. E. Mattson, C. H. Sowers, S. D. Bader, Phys. Rev. B., **48**, 15755 (1993).
[4] T.Y. Chen, S. X. Huang, C. L. Chien, M. D. Stiles, Phys. Rev. Lett., **96**, 207203-1 (2006).
[5] A. E. Berkowitz, J. R. Mitchell, M. J. Carey, A. P. Young, S. Zhang, F. E. Spada, F. T. Parker, A. Hutten, G. Thomas, Phys. Rev. Lett. **68**, 3745 (1992).
[6] Q. Xiao, J. S. Jiang. C. L. Chien, Phys. Rev. Lett., **68**, 3749 (1992).
[7] L. Berger, Phys. Rev. B., **54**, 9353 (1996).
[8] J. C. Slonczewski, J. Magn. Magn. Mate., **159**, L1 (1996).
[9] J. Grollier, V. Cross, A. Hamzic, J. M. George, H. Jaffres, A. Fert, G. Faini, J. Ben Youssef, H. Legall, Appl. Phys. Lett., **78,** 3663 (2001).
[10] J. A. Katine, F. J. Albert, R. A. Buhrman, E. B. Myers, D. C. Ralph, Phys. Rev. Lett. **84,** 3149 (2000).
[11] S. I. Kiselev, J. C. Sankey, I. N. Krivorotov, N. C. Emley, R. J. Schoelkopf, R. A. Buhrman, D. C. Ralph, Nature (London), **425**, 380 (2003).
[12] T. Suzuki, S. Fukami, K. Nagahara, N. Ohshima, N. Ishiwata, IEEE Trans. Magn., **44**, 2535 (2008).
[13] E. Gómez, X. Alcobe, E. Vallés, Journal of Electroanalytical Chemistry, **505**, 54 (2001).
[14] I. Bakonyi, L. Péter, Progress in Materials Science, **55**, 107 (2010).
[15] I. Horcas, R. Fernández, J. Gómez, M. Rodríguez, J. Colchero, J. Gómez-Herrero, A. M. Baro, Rev. Sci. Instrum., **78**, 013705-1 (2007).
[16] T. Luciński, J. Magn. Magn. Mate., **219**, 303 (2000).
[17] F. J. Albert, J. A. Katine, R. A. Buhrman, D. C. Ralph, Appl. Phys. Lett., **77**, 3809 (2000).
[18] J. Z. Sun, D. J. Monsma, D. W. Abraham, M. J. Rooks, R. H. Koch, Appl. Phys. Lett., **81**, 2202 (2002).

*Corresponding authors: pascariu_petronela@yahoo.com